Plasma Sources Sci. Technol. **6** (1997) 437–449. Printed in the UK PII: S0963-0252(97)85884-7

Modelling plasma discharges at high electronegativity

A J Lichtenberg†, I G Kouznetsov†, Y T Lee†§, M A Lieberman†, I D Kaganovich‡ and L D Tsendin‡

† Department of Electrical Engineering and Computer Sciences and the Electronics Research Laboratory, University of California, Berkeley, CA 94720, USA
‡ Physical Technical Department, St Petersburg State Technical University, 195251, Russia

Received 14 January 1997, in final form 30 June 1997

Abstract. Macroscopic models for the equilibrium of a three-component electronegative gas discharge are developed. Assuming the electrons and the negative ions to be in Boltzmann equilibrium, a positive ion ambipolar diffusion equation is derived. Such a discharge can consist of an electronegative core and may have electropositive edge regions, but the electropositive regions become small for the highly electronegative plasma considered here. In the parameter range for which the negative ions are Boltzmann, the electron density in the core is nearly uniform, allowing the nonlinear diffusion equation to be solved in terms of elliptic integrals. If the loss of positive ions to the walls dominates the recombination loss, a simpler parabolic solution can be obtained. If recombination loss dominates the loss to the walls, the assumption that the negative ions are in Boltzmann equilibrium is not justified, requiring coupled differential equations for positive and negative ions. Three parameter ranges are distinguished corresponding to a range in which a parabolic approximation is appropriate, a range for which the recombination significantly modifies the ion profiles, but the electron profile is essentially flat, and a range where the electron density variation influences the solution. The more complete solution of the coupled ion equations with the electrons in Boltzmann equilibrium, but not at constant density, is numerically obtained and compared with the more approximate solutions. The theoretical considerations are illustrated using a plane parallel discharge with chlorine feedstock gas of p = 30, 300 and 2000 mTorr and $n_{e0} = 10^{10}$ cm^{-3}, corresponding to the three parameter regimes. A heuristic model is constructed which gives reasonably accurate values of the plasma parameters in regimes for which the parabolic profile is not adequate.

1. Introduction

We are concerned with the equilibrium plasma quantities, and their scaling with external parameters, of electronegative plasma discharges which are commonly used for plasma processing. In an early study of an electronegative positive column the continuity and force equations for a three species plasma, consisting of electrons, one positive and one negative ion species, were solved numerically to obtain the equilibrium for a positive column [1]. However, the numerical results gave little insight into the importance of various terms in the equations and to the scaling with parameters. Recent work has attempted to analyse such plasmas, using various simplifications to make the calculations more tractable and to uncover the important scalings [2–7].

A procedure for simplifying the analysis, which also uncovered the basic structure of the discharge was developed by Tsendin [3] to treat a cylindrical dc discharge. In that work it was recognized that the discharge would naturally stratify into two regions, an electronegative core in which essentially all of the negative ions would concentrate and an electropositive edge. The physical mechanism of this stratification was investigated in [4]. However, the resulting equations were still quite complicated such that further simplifications were required for analysis. In particular, detachment rather than recombination was considered as the main process for removing negative ions, thus linearizing the coupled equations. The usually more important process of recombination was considered briefly in [3], and in more detail in [6].

In another approach, Lichtenberg *et al* [7] further reduced the problem by using the approximation that the negative ions, as well as the electrons, are in Boltzmann equilibrium. In this situation the electron profile is nearly constant, and a single ambipolar diffusion equation can be constructed to describe the equilibrium. Approximate solutions can be constructed if the core electronegative

§ Work performed while on leave from the Lawrence Livermore National Laboratory.

region and the edge electropositive region have constant (but different) ambipolar diffusion coefficients. The approximations are particularly suited to the parameter regime in which the loss of positive ions to the walls dominates the recombination loss. The analysis was applied to a large aspect ratio oxygen discharge at relatively low density and relatively high pressure, in which dissociation of O_2 is not important.

In many electronegative plasmas more than one positive or negative ion species, as well as neutral species, may be important. The work in [2] was generalized to include more species, but at the expense of obtaining a large set of coupled differential equations that could only be solved numerically [6]. In another approach to the multi-species plasma, one form of a *global model*, in which the negative ions are assumed uniformly distributed over the plasma, was developed [8]. We shall extend this definition of a global model more generally below. A global model is particularly useful in determining the effects of various species, by setting the corresponding reaction rates to zero, which gives information required to obtain the most relevant reduced set of species and reactions.

In this paper previous work on three-species spatially nonuniform plasma is extended to higher electronegativity, in which the positive–negative ion recombination may dominate the diffusive flow and for which the basic assumption of Boltzmann negative ions may not hold. The electronegative plasma is also limited by the restriction that the local positive ion diffusion velocity cannot exceed a local ion sound velocity [9]. The assumption of a parabolic negative ion density profile in the electronegative region reduces the problem to a set of coupled algebraic equations from which rather straightforward numerical results can be obtained. We then introduce a global model, in which the scale length of the parabola is equal to the plasma length, and show that this model approximates the more complete solution, in a limited region of relatively high electronegativities.

However, when recombination loss dominates the ion flux to the walls, the Boltzmann assumption does not hold for negative ions. In this regime a pair of differential equations can be obtained under the assumption of Boltzmann electrons. We show that there is an intermediate electronegativity regime in which the negative ions are not Boltzmann, but the electron density profile is quite flat. We can then recover an elliptic integral solution to a single differential equation, but with different coefficients to those in the lower electronegativity regime. A parabolic profile becomes an increasingly poor approximation to the elliptic profile as the electronegativity increases. A second transition occurs to a regime in which the spatial variation of the electron density cannot be ignored, and the coupled differential equations must then be solved as an eigenvalue problem. We will estimate these two transitions, and compare the results of various approximations in the various regimes.

In this study we are concerned only with the equilibrium discharge properties and do not consider either heating mechanisms or sheaths. The equilibrium discharge properties can be combined with the heating and sheath properties to obtain a complete discharge model [10]. We have used an approximate global model, justified in this paper, to develop a complete discharge model at high electronegativity [11].

2. Physical model

As in previous work, we consider a plasma of three charged particle species: positive ions of density n_+, negative ions of density n_- and electrons of density n_e. For simplicity we consider the spatial variation in a 1D (slab) geometry. For each charged species we have a flux equation

$$\Gamma_i = -D_i \nabla n_i \pm n_i \mu_i E \tag{1}$$

where $D_i = eT_i/m_i\nu_i$, $\mu_i = |q_i|/m_i\nu_i$, with ν_i the total momentum transfer collision frequency, E the electric field, T_i the species temperature in voltage units, q_i the electric charge, and $\pm$ corresponds to positive and negative carriers, respectively. In this approximation we consider the pressure to be sufficiently high that a constant mobility model is appropriate, but not so high that the electron temperature becomes nonuniform. We form a set of coupled differential equations using the continuity equations for each species

$$\nabla \cdot \Gamma_i = S_i \tag{2}$$

where S_i are the sources and sinks, together with a relation for the electric field (Poisson's equation or charge neutrality), and an assumption that the T_i are known. The absence of a stationary current gives

$$\sum_{i=1}^{N} q_i \Gamma_i = 0. \tag{3}$$

We will not formulate a complete general description here. Since the electrons are very mobile, in the bulk plasma we eliminate the electric field by use of a Boltzmann assumption for the electrons

$$D_e \nabla n_e + \mu_e n_e E = 0 \tag{4}$$

which holds except for very high ratio of ion density to electron density, $\alpha \gg \mu_e/\mu_-$, which is not considered in this paper.

At high electronegativity the negative ions are not generally in Boltzmann equilibrium with the potential. The combination of flux equations (1) and the continuity equations (2) results in a pair of differential equations which in 1D (plane parallel geometry) is

$$\frac{\mathrm{d}}{\mathrm{d}x}\left(-D_+\frac{\mathrm{d}n_+}{\mathrm{d}x} + n_+\mu_+E\right) = K_{iz}n_0n_e - K_{rec}n_+n_- \tag{5}$$

and

$$\frac{\mathrm{d}}{\mathrm{d}x}\left(-D_-\frac{\mathrm{d}n_-}{\mathrm{d}x} - n_-\mu_-E\right) = K_{att}n_0n_e - K_{rec}n_+n_- \tag{6}$$

where n_0 is the neutral gas density, K_{iz} is the ionization rate constant, K_{rec} is the recombination rate constant,

K_{att} is the dissociative attachment rate constant, and we have only retained the dominant reactions. The electric field and the density of one species may be eliminated using the Boltzmann relation for electrons and the plasma approximation of charge neutrality. Making these substitutions and taking $D_- = D_+$ and $\mu_- = \mu_+$ for simplicity, we obtain

$$\frac{\mathrm{d}}{\mathrm{d}x}\left(-D_+\frac{\mathrm{d}}{\mathrm{d}x}(n_- + n_e) - \mu_+(n_- + n_e)\frac{D_e}{\mu_e}\frac{1}{n_e}\frac{\mathrm{d}n_e}{\mathrm{d}x}\right) = K_{iz}n_0n_e - K_{rec}(n_- + n_e)n_- \tag{7}$$

$$\frac{\mathrm{d}}{\mathrm{d}x}\left(-D_+\frac{\mathrm{d}n_-}{\mathrm{d}x} + \mu_+n_-\frac{D_e}{\mu_e}\frac{1}{n_e}\frac{\mathrm{d}n_e}{\mathrm{d}x}\right) = K_{att}n_0n_e - K_{rec}(n_- + n_e)n_-. \tag{8}$$

Equations (7) and (8) can be solved simultaneously, together with the appropriate boundary conditions, to obtain the density profiles. We will do this numerically after obtaining simpler equation sets for the various regimes.

If we make the restrictive assumption that the negative ion species is in Boltzmann equilibrium, then

$$\frac{\nabla n_-}{n_-} = \gamma\frac{\nabla n_e}{n_e} \tag{9}$$

where $\gamma = T_e/T_i$ (T_i is the common temperature of the ionic species), then using (1), (3), (4) and (9) together with charge neutrality and the Einstein relations, and assuming a single positive ion species, we obtain an approximate ambipolar diffusion coefficient for the positive ions [12]

$$D_{a+} \simeq D_+\frac{1 + \gamma + 2\gamma\alpha}{1 + \gamma\alpha}. \tag{10}$$

The structure of D_{a+} is easily seen from (10). For $\alpha \gg 1$, γ cancels such that $D_{a+} \approx 2D_+$. When α decreases below 1, but $\gamma\alpha \gg 1$, $D_{a+} \approx D_+/\alpha$ such that D_{a+} increases inversely with decreasing α. For $\gamma\alpha < 1$, $D_{a+} \approx \gamma D_+$, which is the usual ambipolar diffusion without negative ions. For plasmas in which $\alpha \gg 1$ at the plasma centre, the entire transition region takes place over a small range of $1/\gamma < \alpha < 1$, such that the simpler value of $D_{a+} = 2D_+$ may hold over most of the electronegative plasma core.

Using (10), the steady-state positive ion continuity equation $\nabla\cdot\Gamma_i =$ source is, in 1D,

$$-\frac{\mathrm{d}}{\mathrm{d}x}\left(D_{a+}(\alpha)\frac{\mathrm{d}n_+}{\mathrm{d}x}\right) = K_{iz}n_0n_e - K_{rec}n_+n_-. \tag{11}$$

We can substitute for n_e and n_- using the Boltzmann relation relating electron and ion densities $(n_e/n_{e0}) = (n_-/n_{-0})^{1/\gamma}$ and the plasma approximation of charge neutrality $n_+ = n_- + n_e$, to obtain

$$n_+ = n_- + n_{e0}\left(\frac{n_-}{n_{-0}}\right)^{1/\gamma}. \tag{12}$$

Substituting (12) into (11), we obtain the ion diffusion equation in terms of α alone

$$-\frac{\mathrm{d}}{\mathrm{d}x}\left[D_{a+}(\alpha)\frac{\mathrm{d}}{\mathrm{d}x}\left((\alpha+1)\left(\frac{\alpha}{\alpha_0}\right)^{\frac{1}{\gamma-1}}\right)\right] = K_{iz}n_0\left(\frac{\alpha}{\alpha_0}\right)^{\frac{1}{\gamma-1}} - K_{rec}n_{e0}\alpha(\alpha+1)\left(\frac{\alpha}{\alpha_0}\right)^{\frac{2}{\gamma-1}} \tag{13}$$

where $D_{a+}(\alpha)$ is given by (10). Because $\gamma \gg 1$ we see from (12) that $n_e \simeq n_{e0}$ in the plasma so that we can generally let $(\alpha/\alpha_0)^{\frac{1}{\gamma-1}} = 1$ in (13).

Equation (13) has as a boundary condition at the sheath edge $x = \ell_p$ that the ion flow cannot exceed the local ion sound velocity, which at the plasma edge is the Bohm velocity. Stating this condition as an equality, it becomes the Bohm flux condition

$$-D_{a+}\left.\frac{\mathrm{d}n_+}{\mathrm{d}x}\right|_{x=\ell_p} = n_+(\ell_p)u_B(T_e,\ T_i,\ \alpha). \tag{14}$$

Here $\alpha = \alpha(\ell_p) = n_-(\ell_p)/n_e(\ell_p)$. Since negative ions may be present when (14) is satisfied, the Bohm velocity has the more general form [13]

$$u_B = \left[\frac{eT_e(1+\alpha)}{M_+(1+\gamma\alpha)}\right]^{1/2} \tag{15}$$

which reduces to the usual expression $u_{B0} = (eT_e/M_+)^{1/2}$ when $\alpha = 0$. For $\alpha > 1/\gamma$ a negative ion density at the sheath edge significantly reduces the Bohm velocity.

Equation (13) can be characterized by three parameters: $\alpha_0 = n_{-0}/n_{e0}$ (the ratio of n_- to n_e at the plasma centre), n_{e0}, and T_e. We can determine these three constants by solving (13) and two particle conservation equations, which are the integrated forms of (2), and an energy conservation equation.

The conservation equations are: positive ion particle balance

$$-D_{a+}\left.\frac{\mathrm{d}n_+}{\mathrm{d}x}\right|_{x=\ell_p} = \int_0^{\ell_p} K_{iz}n_0n_e\mathrm{d}x - \int_0^{\ell_p} K_{rec}n_+n_-(n_+)\mathrm{d}x \tag{16}$$

negative ion particle balance

$$\int_0^{\ell_p} K_{att}n_0n_e\mathrm{d}x - \int_0^{\ell_p} K_{rec}n_+n_-(n_+)\mathrm{d}x = 0 \tag{17}$$

and energy balance

$$P_{abs} = 2\mathcal{E}_c\int_0^{\ell_p} K_{iz}n_0n_e\mathrm{d}x + 2\mathcal{E}_w n_+(\ell_p)u_B \tag{18}$$

where $\mathcal{E}_c(T_e)$ is the collisional energy lost per electron–positive ion pair created, and $\mathcal{E}_w$ is the kinetic energy lost to the wall per electron–ion pair lost to the wall. Given the neutral density n_0 and the power per unit area deposited in the electrons, P_{abs}, the three equations can be simultaneously solved for the three unknowns T_e, α_0 and n_{e0}, provided ℓ_p is known. The plasma half width ℓ_p differs from the half length of the device by a sheath width s. In a complete model we must determine s self-consistently with ℓ_p, given the discharge heating mechanism. A common assumption is that $s \ll \ell_p$. The set of equations (13)–(18) can only be solved numerically such that the underlying scaling laws cannot be easily uncovered. However, we shall see in the next section that various reasonable approximations allow analytic solutions to be obtained.

We now examine the condition for validity of the Boltzmann equilibrium for negative ions. From (1), for negative ions, we have

$$\Gamma_- = -D_- \frac{\mathrm{d}n_-}{\mathrm{d}x} - n_-\mu_- E \tag{19}$$

with the condition for Boltzmann equilibrium, as in (4), being that

$$\left|\Gamma_- \Big/ \left(D_- \frac{\mathrm{d}n_-}{\mathrm{d}x}\right)\right| \ll 1 \tag{20}$$

everywhere. Using the integral relation between the source and the flux, as in (17), Γ_- can be written as

$$\Gamma_- = \int_0^x K_{att} n_0 n_e \mathrm{d}x - \int_0^x K_{rec} n_+ n_- \mathrm{d}x. \tag{21}$$

If we have profiles for n_e, n_- and n_+, (21) can be explicitly evaluated, as we shall do in the next section. Since the recombination increases with the square of the density, at high density (20) is no longer satisfied. We can estimate the left hand side (LHS) of (20), using (21) and the solution which holds when (20) is satisfied. We have done this in section 3, finding a parabolic solution. Using (21) we find that (20) has its maximum value at $x = 0$, giving the condition for which negative ions are in Boltzmann equilibrium

$$\rho \equiv \frac{7}{30} K_{rec} n_{e0} \alpha_0 \ell_p^2 \big/ D_- < 1. \tag{22}$$

Since the LHS in (22) is the largest value that the LHS in (20) attains, we have used a simple, rather than a strong inequality in (22).

If (22) is not satisfied, the negative ions are not in Boltzmann equilibrium and equation (13) is not valid, but the electron profile may still be quite flat, which also allows the reduction to a single differential equation for the profile. Using (19) and (21), beyond this transition, we have

$$n_-\mu_- E(x) = -\left(\int_0^x K_{att} n_0 n_{e0} \mathrm{d}x - \int_0^x K_{rec} n_+ n_- \mathrm{d}x + D_- \frac{\mathrm{d}n_-}{\mathrm{d}x}\right). \tag{23}$$

The electric field is now determined implicitly in terms of integrals over the source terms plus a usually small gradient correction. Because $T_e \gg T_i$, there is a large parameter range in which (22) is not satisfied but n_e is still essentially flat, as determined by the Boltzmann relation. To determine this condition explicitly, we first assume that all terms involving variation of n_e are negligible. Then we can substitute (23) into equation (5) for positive ions and, using the approximation that $n_- \simeq n_+$ ($n_e \ll n_-$), and dropping small terms, we obtain

$$\frac{\mathrm{d}}{\mathrm{d}x}\left[-\left(1 + \frac{T_-}{T_+}\right) D_+ \frac{\mathrm{d}n_+}{\mathrm{d}x} + r_\mu \int_0^x K_{rec} n_+^2 \mathrm{d}x - r_\mu \int_0^x K_{att} n_0 n_e \mathrm{d}x\right] \simeq K_{iz} n_0 n_e - K_{rec} n_+^2 \tag{24}$$

where $r_\mu = \mu_+/\mu_-$. We evaluate the LHS to obtain,

$$\left(1 + \frac{T_-}{T_+}\right) D_+ \frac{\mathrm{d}^2 n_+}{\mathrm{d}x^2} + (K_{iz} + r_\mu K_{att}) n_0 n_e - (1 + r_\mu) K_{rec} n_+^2 = 0. \tag{25}$$

Equation (25) has an elliptical integral solution, which we obtain in subsection 3.3.

To determine the condition for (25) to be valid we add (7) and (8). Dropping small terms, we obtain

$$\frac{\mathrm{d}}{\mathrm{d}x}\left(-2D_+ \frac{\mathrm{d}n_-}{\mathrm{d}x} - \gamma D_+ \frac{\mathrm{d}n_e}{\mathrm{d}x}\right) = (K_{iz} + K_{att}) n_0 n_e - 2K_{rec} n_+^2 \tag{26}$$

where we have used the Einstein relation to write $\mu_+ D_e/\mu_e = \gamma D_+$. Equation (26) is still a function of two variables n_e and n_- so that a simplified form of (7) or (8) would be required to be solved simultaneously with (26) to obtain a general solution. Comparing (26) with (25) we see that (25) is just the approximation that the electron gradient term in (26) can be dropped for the simplified case with $r_\mu = 1$ and $T_-/T_+ = 1$. From (26) we would expect that with increasing ρ the ionization and attachment are increasingly balanced locally by the recombination. In this regime the LHS is a perturbation to the RHS, the RHS on its own gives the proportionality

$$n_e \propto n_-^2 \ (\alpha \gg 1, \text{ and high pressure})$$

which is quite different from the parameters for which $n_e \simeq n_{e0}$, a constant, with n_- varying with position. However, both n_e and n_- may only vary slightly over the bulk discharge (see our examples in section 4). A complete solution requires the simultaneous solution of (7) and (8).

Using the same procedure that we employed to obtain (22) for the validity of a parabolic solution, we now obtain the condition for validity of the elliptic solution. This is more difficult since we need to expand the elliptic solution at the origin and, unlike the parabolic solution the gradient for the elliptic solution, is much flatter and varies greatly with changing parameters. We present the calculation in an appendix, using the elliptic solution found in subsection 3.3. The result, from equation (A19), is

$$\kappa \equiv \frac{1}{11.55\alpha_0}\left(\frac{D_+}{K_{rec} n_{e0} \alpha_0 \ell_p^2}\right)^{1/2} \times \exp\left(\frac{2K_{rec} n_{e0} \alpha_0 \ell_p^2}{D_+}\right)^{1/2} < 1. \tag{27}$$

The exponential dependence with increasing recombination is the result of the flattening of the elliptic solution with increasing recombination.

We shall compare the results obtained from the parabolic and elliptic solutions, using conditions (22) and (27), with numerical solutions of the coupled equations in section 4. First we develop the approximate parabolic and elliptic solutions.

3. Approximate solutions

3.1. The parabolic approximation

Consider first that a central region of the discharge exists in which α is large, and the negative ions are in approximate Boltzmann equilibrium, i.e. (22) is satisfied, then $n_e \simeq n_{e0}$, a constant, and $D_{a+} \simeq$ constant except near the edge of the region. The differential equation (5) becomes

$$-D_{a+}\frac{\mathrm{d}^2 n_+}{\mathrm{d}x^2} = K_{iz} n_0 n_{e0} - K_{rec} n_+ n_-. \qquad (28a)$$

Noting that $n_- = \alpha n_{e0}$ and $n_+ = (1+\alpha)n_{e0}$, we can rewrite (28a) in terms of the single variable α

$$-D_{a+}\frac{\mathrm{d}^2 \alpha}{\mathrm{d}x^2} = K_{iz} n_0 - K_{rec} n_{e0}(1+\alpha)\alpha. \qquad (28b)$$

We have not used the approximation that $n_- = n_+$ in the source term, as it is unnecessary, and the present form connects our expressions to previous lower α solutions [7, 9]. If the flow dominates the recombination, then the effect of positive–negative ion recombination can be neglected in determining the spatial profile (but not the plasma parameters). The diffusion equation (28) then takes the simple form

$$-D_{a+}\frac{\mathrm{d}^2 n_+}{\mathrm{d}x^2} = K_{iz} n_0 n_{e0}.$$

Assuming D_{a+} is constant, then $n_+(x)$ has a parabolic solution

$$\frac{n_+}{n_{e0}} = \frac{n_-}{n_{e0}} + 1 = \alpha_0\left(1 - \frac{x^2}{\ell^2}\right) + 1 \qquad (29)$$

where the point $x = \ell$ corresponds to a zero of n_-, $\ell \neq \ell_p$ which must be found. In previous work [7], at relatively small α, with $\rho < 1$, $\ell < \ell_p$ and the central electronegative solution is matched to an electropositive edge solution. However, at relatively high α (but $\rho < 1$) the electropositive edge becomes small and, according to our previous results, the electronegative region may join onto a non-neutral sheath with a Bohm velocity as given by (15). In this case $\ell > \ell_p$ and $n_- > 0$ at the plasma–sheath boundary. Anticipating that we are considering this case, we make the assumption in (29) that the scale length $\ell > \ell_p$, and that the electronegative region extends to the plasma edge. This corresponds to a profile truncated at the plasma–sheath edge (see below for further discussion of this assumption). The particle balance equation for positive ions is then

$$K_{iz} n_0 n_{e0} \ell_p = K_{rec} n_{e0}^2 \left\{ \alpha_0^2 \ell_p \left(1 - \frac{2}{3}\frac{\ell_p^2}{\ell^2} + \frac{1}{5}\frac{\ell_p^4}{\ell^4}\right) + \alpha_0 \ell_p \left(1 - \frac{1}{3}\frac{\ell_p^2}{\ell^2}\right)\right\} + n_{e0}\left[\alpha_0\left(1 - \frac{\ell_p^2}{\ell^2}\right) + 1\right] u_B(\alpha) \qquad (30)$$

where $u_B(\alpha)$ is given by (15) with

$$\alpha = \alpha_0\left(1 - \frac{\ell_p^2}{\ell^2}\right). \qquad (31)$$

For the higher α cases the second term in the curly braces can be neglected. The negative ion particle balance is

$$K_{att} n_0 n_{e0} \ell_p = K_{rec} n_{e0}^2 \left\{ \ \cdot \ \right\} \qquad (32)$$

with the $\{\ \cdot\ \}$ repeated from (30). The third equation to complete the set is matching the positive ion edge diffusion flux to the Bohm flux

$$2 D_{a+} \alpha_0 n_{e0} \frac{\ell_p}{\ell^2} = n_{e0}\left[\alpha_0\left(1 - \frac{\ell_p^2}{\ell^2}\right) + 1\right] u_B(\alpha). \qquad (33)$$

For reasonably high α, from (10) we can set

$$D_{a+} = (1 + T_-/T_+) D_+.$$

Then, given n_{e0} and ℓ_p, the three equations (30), (32) and (33) can be solved simultaneously for α_0, T_e, and ℓ. If the power is given, rather than n_{e0}, then (18) gives the additional equation for n_{e0}.

Examining the above equations we see that the terms in the curly braces arise from integrations over a profile and are therefore less sensitive to the profile. The third term on the RHS of (30), the Bohm flux, is sensitive to ℓ_p^2/ℓ^2, but for large α tends to be small compared to the volume terms, so the sensitivity is not as critical. In (33) the LHS does not depend critically on the edge region, in which D_{a+} may vary significantly, because it is an integrated flux which remains relatively constant. Some care must be taken, however, in treating the RHS of (33) as we see below. The truncation of the parabolic profile at $x = \ell_p$ ($\ell > \ell_p$) is not exact, but does follow the expected steepening of the edge profile in a more complete solution. The insensitivity of the integrals to profile variations also justifies the extended use of (29) to a region in which (22) may be marginally not satisfied. Comparing (28) to (25), with $D_{a+} = (1 + T_-/T_+)D_+$, we see that the two become equal if we set $K_{att} n_0 n_e = K_{rec} n_+^2$. Although this is never strictly true, it is true in an average sense, over the plasma, as required by negative ion particle balance, from (17). Thus once the profile is specified the integrated equations give identical results.

The equation set, given above, can be simplified in the following ways. For $\alpha_0 \gg 1$, we keep only the terms quadratic in α_0 in (32),

$$\alpha_0 = \left(\frac{K_{att} n_0}{K_{rec} n_{e0}}\right)^{1/2} \left(1 - \frac{2}{3}\frac{\ell_p^2}{\ell^2} + \frac{1}{5}\frac{\ell_p^4}{\ell^4}\right)^{-1/2}. \qquad (34a)$$

Since we generally find that $\ell/\ell_p \approx 1$, an estimate of α_0 is

$$\alpha_0 \approx \left(\frac{15}{8}\frac{K_{att} n_0}{K_{rec} n_{e0}}\right)^{1/2} \qquad (34b)$$

which gives the important square root scaling $n_- \propto (n_0 n_{e0})^{1/2}$. The temperature dependence in (34) is weak, with T_e essentially clamped by the strong T_e dependence of K_{iz} in (30). Given an approximate value of α_0 from (34), the ratio ℓ_p/ℓ can be obtained from the Bohm criterion (33).

For $\alpha_0\left(1-\frac{\ell_p^2}{\ell^2}\right) \gg 1$, we have the edge flux condition, from (33),

$$\frac{4D_+\alpha_0 n_{e0}\ell_p}{\ell^2} = n_{e0}\alpha_0\left(1-\frac{\ell_p^2}{\ell^2}\right)u_B(\alpha) \qquad (35)$$

where we have used $T_- = T_+ \equiv T_i$. A simple estimate of ℓ is possible for this case. Substituting for $u_B(\alpha)$ and dropping small terms, (35) becomes

$$\ell_p^2/\ell^2 = 1 - \frac{4\lambda}{\left(\frac{\pi}{8}\right)^{1/2}\ell_p}. \qquad (36)$$

where we have substituted the ion mean free path λ for $D_+/(8eT_i/\pi M_+)^{1/2}$. For the higher pressure plasmas at which α_0 is large (see the scaling in (34)) $\lambda/\ell_p \ll 1$, justifying an approximation of $\ell_p/\ell \simeq 1$.

Since (36) indicates that $\ell_p/\ell \simeq 1$, we can use a simplified model for which $\ell_p/\ell \equiv 1$, which we call a *global model*. In the global model (30) and (32) reduce to

$$K_{iz}n_0\ell_p = \frac{8}{15}K_{rec}n_{e0}\alpha_0^2\ell_p + 2(1+T_-/T_+)D_+\alpha_0/\ell_p \quad (37a)$$

$$K_{att}n_0 = \frac{8}{15}K_{rec}n_{e0}\alpha_0^2 \qquad (37b)$$

where we have, for simplicity, dropped the term linear in α_0 and have used (33) to substitute the known edge flux for the Bohm condition within the global approximation. As a first estimate, we can reduce (37*a*) by recognizing that if the recombination loss dominates the flux to the wall, then the last term in (37*a*) can be dropped, and substituting from (37*b*) we have the very simple result for obtaining T_e,

$$K_{iz} \simeq K_{att} \qquad (37c)$$

which is independent of the parabolic approximation.

The single region parabolic approximation for the range of parameters in which (22) is satisfied is then to solve (30), (32) and (33), for α_0, T_e, and ℓ. For $\alpha_0(1-\ell_p^2/\ell^2) \gg 1$ we can use the simpler set (36), (37*b*) and a simplified form of (30). The equation set is further reduced to two equations in the approximation of a global model with $\ell = \ell_p$. In this model (37*b*) is solved together with (37*a*) for α_0 and T_e.

3.2. The electropositive edge

As mentioned above, there is most generally an edge electropositive region which becomes small as α becomes large. This region can be included directly into the theory by introducing another parameter l_- specifying the electropositive edge region, and an additional equation for the edge region. We can then formulate the criterion for which the electropositive region disappears. First we find a simple equation for the edge region by noting that in the higher electric fields of the edge the negative ions are swept rapidly into the bulk, such that the recomination can be ignored. From (26), dropping the small terms, the electropositive edge is governed by the equation [3]

$$-\gamma D_+\frac{d^2 n_e}{dx^2} = (K_{iz}+K_{att})n_0 n_e \qquad (38)$$

with a solution of the form

$$n_e = A\cos\left[\left(\frac{(K_{iz}+K_{att})n_0}{\gamma D_+}\right)^{1/2}(x-\ell_-)+B\right] \qquad (39)$$

where $n_e \simeq n_+$ in this region. The constants A and B are determined from the conditions that $n_e(\ell_-) = n_{e0}$ and flux continuity $\Gamma_+(\ell_-) = -\gamma D_+ \left.\frac{dn_e}{dx}\right|_{x=\ell_-}$. The parabolic approximation for the central region is generalized to the form

$$n_+ = \alpha_0 n_{e0}\left(1-\frac{\ell_-^2}{\ell^2}\right) + n_{e0}. \qquad (40)$$

The electropositive edge continuity equation for ℓ_- is

$$\Gamma_+(\ell_-) + K_{iz}n_0\int_{\ell_-}^{\ell_p} n_e(x)dx = u_B(T_e)n_e(\ell_p) \qquad (41)$$

where $n_e(x)$ is obtained from (39), and $u_B(T_e) = [eT_e/M_+]^{1/2}$.

Since we are interested in high α, where $(\ell_p-\ell_-)/\ell_p$ is usually small, we estimate the size of the electropositive region from a perturbation analysis. Taking $\ell_- \simeq \ell_p$ then the parabolic solution gives the edge α, such that

$$\Gamma_+(\ell_-) \simeq u_B(\alpha)\alpha n_{e0}. \qquad (42)$$

Solving for the constants A and B in (39), using (42), substituting the result into (41), with $u_B(\alpha) \simeq u_{B0}/\gamma^{1/2}$, from (15), and keeping only terms linear in $\delta\ell \equiv \ell_p - \ell_-$, we obtain

$$\frac{\delta\ell}{\ell_p} = \frac{1-\alpha/\gamma^{1/2}}{\frac{\alpha}{\gamma^{1/2}}\frac{u_{B0}\ell_p}{\gamma D_+} + \frac{K_{iz}n_0\ell_p}{u_{B0}}}. \qquad (43)$$

For high K_{iz} and K_{att} (high α), $\delta\ell/\ell_p \ll 1$ and goes to zero for $\Gamma_+(\ell_-) = u_{B0}n_{e0}$ which occurs, as seen in (43), when

$$\alpha(\ell_-) = \gamma^{1/2}. \qquad (44)$$

At this point the electropositive edge region disappears.

3.3. The elliptic approximation

If (22) is not satisfied the central region flattens and the edge steepens, so that a parabolic approximation is not adequate. If (27) is satisfied equation (25) holds. We transform (25) to a form which can be solved in terms of elliptic integrals. Reintroducing the product n_+n_- into the recombination term and writing $n_+n_- = n_{e0}^2\alpha(\alpha+1)$ we transform (25) to

$$-\frac{1}{2(1+T_-/T_+)D_+n_{e0}}\frac{d}{d\alpha}\beta^2$$
$$= (K_{iz}+r_\mu K_{att})n_0 n_{e0} - (1+r_\mu)K_{rec}n_{e0}^2\alpha(\alpha+1) \quad (45)$$

where we have used the chain rule, and

$$\beta(\alpha) = -(1+T_-/T_+)D_+n_{e0}\frac{d\alpha}{dx}. \qquad (46)$$

We can integrate (45) once, over α, and using the boundary condition that $\beta(\alpha_0) = 0$ we obtain

$$\beta(\alpha) = \beta_0\left[(\alpha_0 - \alpha) - \frac{(1+r_\mu)K_{rec}n_{e0}}{(K_{iz}+r_\mu K_{att})n_0} \times\left(\frac{\alpha_0^3-\alpha^3}{3} + \frac{\alpha_0^2-\alpha^2}{2}\right)\right]^{1/2} \quad (47)$$

with

$$\beta_0 = [2(1+T_-/T_+)D_+(K_{iz}+r_\mu K_{att})n_0 n_{eo}^2]^{1/2}. \quad (48)$$

Rearranging (46) and integrating, we obtain

$$x(\alpha) = \int_{\alpha(x)}^{\alpha_0} \frac{(1+T_-/T_+)D_+n_{e0}\mathrm{d}\alpha}{\beta(\alpha)} \quad (49)$$

where $\beta(\alpha)$ is given by (47). Equation (49) is an elliptic integral, from which, after some algebra, and dropping the small $\sim (1/\alpha_0)$ terms, we obtain

$$x = \frac{(1+T_-/T_+)D_+n_{e0}}{\beta_0}\frac{\alpha_0}{(\eta/3)^{1/2}} \times \int_{\alpha(x)}^{\alpha_0} \frac{\mathrm{d}\alpha}{[(b\alpha_0-\alpha)(\alpha_0-\alpha)(a\alpha_0+\alpha)]^{1/2}} \quad (50)$$

where

$$\eta = \frac{(1+r_\mu)K_{rec}n_{e0}\alpha_0^2}{(K_{iz}+r_\mu K_{att})n_0} \quad (51)$$

$\eta < 1$, and

$$a = \frac{1}{2} + \frac{1}{2}\left(\frac{12}{\eta} - 3\right)^{1/2} \qquad b = -\frac{1}{2} + \frac{1}{2}\left(\frac{12}{\eta} - 3\right)^{1/2}. \quad (52)$$

The integral on the right of (50) is a standard elliptic integral. Using an appropriate boundary condition at ℓ_p gives a relation for one of the unknown constants α_0 or T_e, in terms of the other, with the second constant determined from negative ion balance. In section 4 we compare the profile from (50) to the solution of the coupled equations, for an appropriate pressure where (27) is satisfied.

4. Numerical results

To make a calculation of a particular electronegative plasma equilibrium the reaction rate constants must be known. Furthermore, these rate constants must be consistent with the approximation of a three-component plasma if that approximation is to be used. For this study we take Cl_2 as the feedstock gas because it is more electronegative than the previously studied O_2 in [7]. The rate constants for this gas have been compiled for use in a global model [11]. The size of the rate constants and the results of the model indicate that it is a good approximation to consider that the equilibrium dynamics are controlled by three plasma species and the neutral gas. The important reaction-rate constants for the charged particles are

$$K_{iz} = 9.2 \times 10^{-14}\exp(-12.9/T_e) \quad (53)$$

$$K_{att} = 3.69 \times 10^{-16}\exp[-1.68/T_e + 1.457/T_e^2 - 0.44/T_e^3] \quad (54)$$

$$K_{rec} = 5.10 \times 10^{-14} \quad (55)$$

$$K_{cx} = 1.3 \times 10^{-15}T_i^{1/2} \quad (56)$$

in units of $m^3\ s^{-1}$ with T_e and T_i in volts. The rates correspond to the reactions

$$\begin{aligned} Cl_2 + e &\to Cl_2^+ + 2e \quad \text{(ionization)} \\ Cl_2 + e &\to Cl^- + Cl \quad \text{(dissociative attachment)} \\ Cl_2^+ + Cl^- &\to Cl_2 + Cl \quad \text{(recombination)} \\ Cl_2^+ + Cl_2 &\to Cl_2 + Cl_2^+ \quad \text{(charge exchange)} \end{aligned}$$

The latter is the dominant process for the positive ion diffusion, resulting in a mean free path

$$\lambda(\mathrm{cm}) \simeq 2 \times 10^{14}/n_0\ (\mathrm{cm}^{-3}). \quad (57)$$

We now use the above quantities to compute the plasma parameters for a particular set of cases which might be typical of certain plasma processing discharges, but span the regimes which we wish to investigate. For a benchmark plasma we take $\ell_p = 0.45$ cm, $n_{e0} = 10^{10}$ cm^{-3} and $p = 300$ mTorr. This corresponds to parameters of a capacitive discharge plasma processing device operating at reasonably high power but at a pressure at which α is relatively high. We have subtracted off the nominal sheath widths from the device width. As we shall see, this case corresponds to the intermediate α regime satisfying (27) but not satisfying (22). To investigate the other regimes we also examine cases for which $p = 30$ mTorr and $p = 2$ Torr.

We solve (5) and (6) subject to the boundary conditions that the density gradients are zero at the centre, the negative ion current is zero at the plasma edge and the positive ion current is limited to the Bohm flux (using (15)) at the plasma edge. We take $T_- = T_+ = 300$ K. In figure 1 we give the solution at the lowest pressure, $p = 30$ mT. The density profiles are given in figure 1(a), the current profiles in figure 1(b), and D_{a+}/D_+ in figure 1(c), where $D_{a+} \equiv -\Gamma_+/\frac{\mathrm{d}n_+}{\mathrm{d}x}$. From the density we observe the profiles to be roughly parabolic. From the current we observe that the recombination flux (negative ion flux) is small compared to the diffusion flux ($\sim$ positive ion flux), and from D_{a+}/D_+ we observe that $D_{a+} \simeq 2D_+$, characteristic of the regime in which the negatives ions are in Boltzmann equilibrium. This is in agreement with our prediction from (22) as $\rho = 0.17$. For this case the eigenvalues are $T_e = 2.86$ eV and $\alpha_0 = 24.73$.

In figure 2 we give the same quantities for the intermediate regime of $p = 300$ mTorr. We note, in figure 2(a), the flattened central profiles of positive and negative ions, and the essentially constant electron profile. This is characteristic of the intermediate regime. We find $\rho = 5$, which does not satisfy (22). From (27) we obtain $\kappa = 0.31$ such that the elliptic solution is valid. The current profiles and values of D_{a+}/D_+ are also consistent with the elliptic solution. We find that $D_{a+} \simeq 2D_+$ at the plasma edge, indicating that the generalized Bohm criterion for the flux limitation is appropriate. The eigenvalues are $T_e = 2.27$ eV and $\alpha_0 = 71.9$.

In figure 3 we increase the pressure to $p = 2$ Torr. We note parenthetically that some underlying assumptions of our analysis, such as uniform electron temperature, are probably not satisfied. However, the example is pedagogically useful in illustrating the highest electronegativity regime. From figure 3(a) we observe that

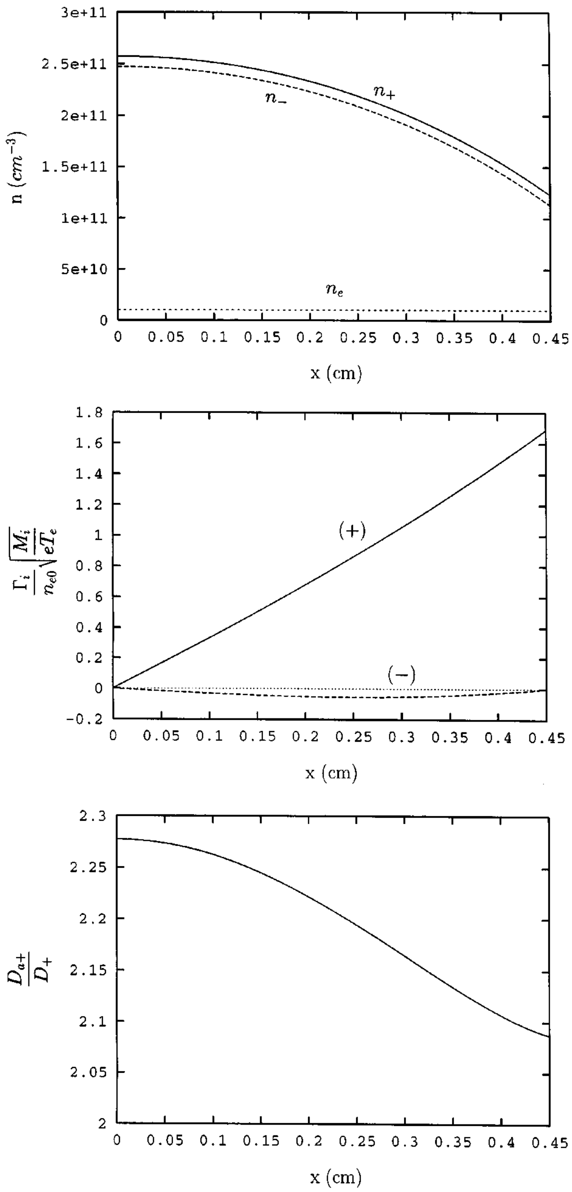

Figure 1. Profiles for a chlorine discharge in one dimension of half length ℓ_p = 0.45 cm, electron density $n_{e0} = 10^{10}$ cm^{-3} and pressure p = 30 mTorr. Top, profiles of the densities n_+, n_- and n_e; middle, profiles of the fluxes Γ_+ and Γ_-; bottom, profile of the diffusion constant ratio D_{a+}/D_+ where $D_{a+} \equiv -\Gamma_+/\frac{dn_+}{dx}$.

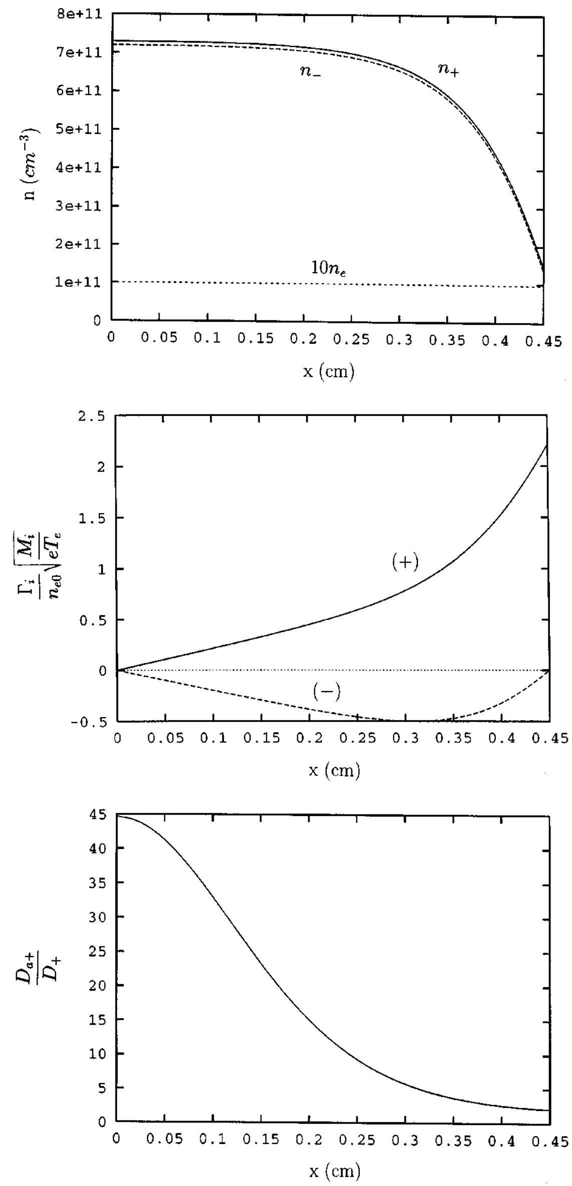

Figure 2. The same as figure 1 for p = 300 mTorr.

n_e is no longer constant. This is consistent with the value of $\kappa \gg 1$. The near equality (with opposite signs) of the positive and negative current, in the plasma bulk, as seen in figure 3(b), indicates that the diffusion terms are small. In figure 3(c), the value of $D_{a+}/D_+ \simeq 2\gamma$ can be shown to be consistent with the proportionality $n_e \propto n_-^2$. However, at the plasma edge we still obtain $D_{a+} \simeq 2D_+$ indicating that the generalized Bohm condition is satisfied.

We now compare the profiles from the first two cases with the simpler approximate solutions. For $p = 30$ mTorr we use (30), (32) and (33), together with (15) for $u_B(\alpha)$ and (31) for α to obtain $T_e = 2.84$, $\alpha_0 = 25.8$ and $\ell/\ell_p = 1.32$. The values are quite close to those obtained in the complete solution and are compared in table 1. For the intermediate pressure case of $p = 300$ mTorr the elliptic integral solution gives $T_e = 2.26$ and $\alpha_0 = 71.5$. Again, these values are quite close to the values obtained from the complete solution, as seen in table 1. In figure 4(a) the parabolic profile for the positive ions is compared to the profile obtained from the coupled equations, for $p = 30$ mTorr. Good profile agreement is found. In figure 4(b) the elliptic profile is compared to the coupled equation profile for $p = 300$ mTorr, again finding that the profiles are reasonably close, as they are predicted to be since (27) is satisfied.

We also note that the parabolic model predicts average quantities quite well at higher pressure, despite the lack of agreement of the profiles. This is illustrated in table 1 by comparing the results from a parabolic model with the better approximations. Although α_0 is too high, as expected, we

Table 1.

	Parabolic profile $u_+(l_p) = u_B$				Elliptic profile $(n(l_p) = 0)$			Coupled equations $(n(l_p) = 0)$		
p(mTorr)	T_e(eV)	α_0	$\bar{\alpha}$	ℓ/ℓ_p	T_e (eV)	α_0	$\bar{\alpha}$	T_e(eV)	α_0	$\bar{\alpha}$
30	2.84	25.8	20.9	1.32				2.86	24.7	20.5
300	2.2	87.5	60.2	1.03	2.26	71.5	63.6	2.27	71.9	63.0
2000	2.14	228.5	152.8	1.003				2.17	170.4	161.8
	Heuristic model									
p(mTorr)	T_e(eV)	α_0	$\bar{\alpha}$	d/ℓ_p						
300	2.25	72.1	63.2	0.43						
2000	2.17	171.6	165.9	0.11						

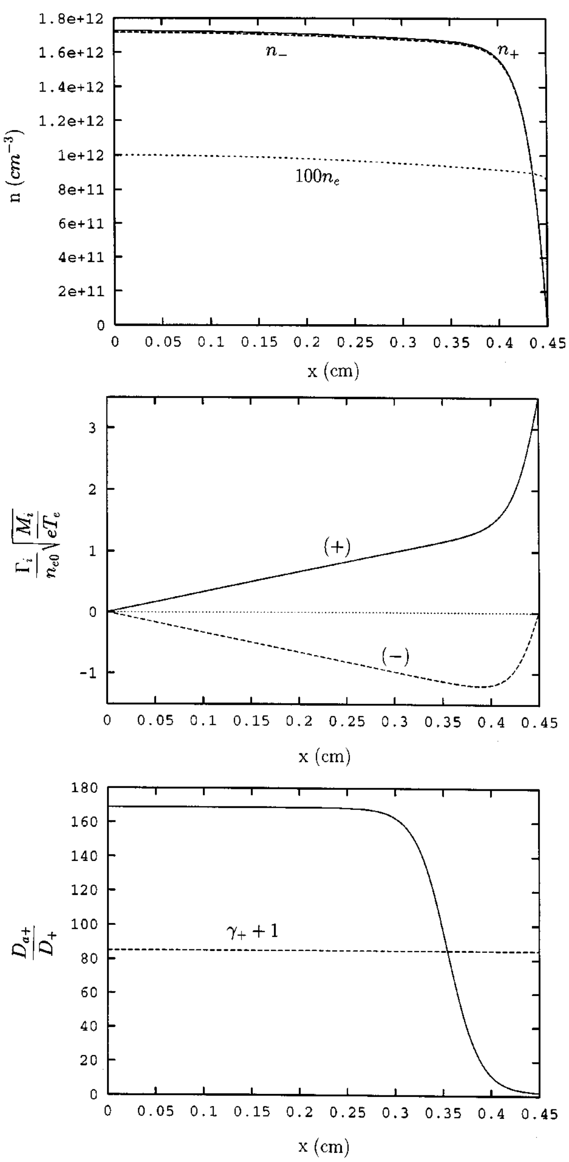

Figure 3. The same as figure 1 for p = 2 Torr.

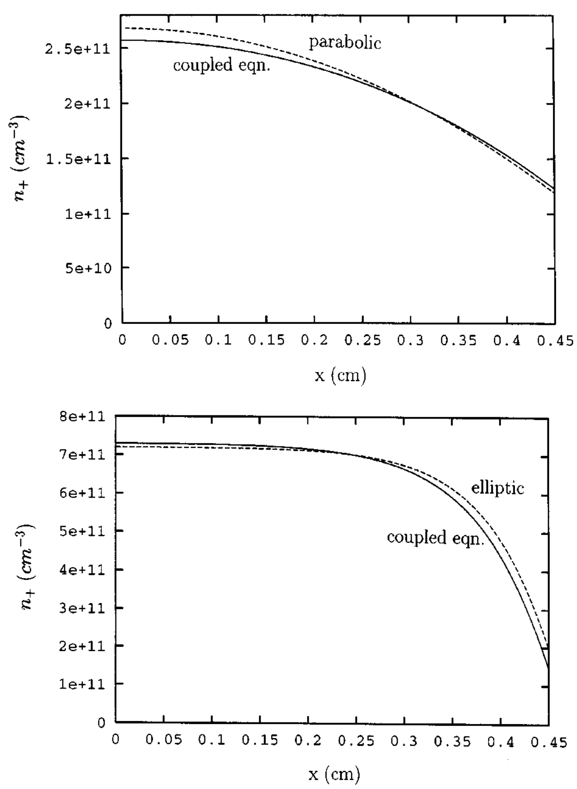

Figure 4. Comparison of n_+ profiles of approximate solutions (dashed curves) to the numerical solutions of the coupled positive and negative ion differential equations (solid curves). Top, parabolic approximate solution at p = 30 mTorr; bottom, elliptic approximate solution at p = 300 mTorr. The other input parameters as in figure 1.

see that the space averaged values of $\bar{\alpha}$ are reasonably close as are the values of T_e. Since $\ell/\ell_p = 1.03$ at $p = 300$, using the parabolic model, we expect that the simpler global model, with $\ell/\ell_p = 1$ will also give approximate values of T_e and $\bar{\alpha}$. A global model is readily solved by a hand calculation, iteratively solving (37a,b). These results are understandable since for the recombination flux dominating the diffusion flux the shape is relatively unimportant.

The important α-scaling with pressure (or electron density) is obtainable, approximately, from (34). Using the square root relation, with the benchmark value of $\bar{\alpha} = 63$ at $p = 300$ mTorr we obtain $\bar{\alpha} = 20$ for $p = 30$ mTorr and $\bar{\alpha} = 163$ for $p = 2$ Torr. These values are reasonably close to the values obtained from the coupled equations, as seen in table 1.

5. A heuristic high-α model

The numerical results of section 4 indicate that the ion density is relatively flat in the central region and drops rather sharply in an increasingly narrow edge region with increasing α_0. A heuristic model that captures this profile is

$$n_+ \simeq n_- = \alpha_0\, n_{e0} \qquad 0 < x < \ell_p - d$$

$$n_+ \simeq n_- = \alpha_0\, n_{e0} \left(1 - \frac{(x + d - \ell_p)^2}{d^2}\right) \qquad \ell_p - d < x < \ell_p. \tag{58}$$

The integrations from $x = 0$ to $x = \ell_p$ from (16) and (17) then yield

$$(K_{iz} n_0 n_{e0} - K_{rec}\alpha_0^2 n_{e0}^2)\ell_p + \frac{7}{15} K_{rec}\alpha_0^2 n_{e0}^2 d = \Gamma_+(\text{wall}) \tag{59}$$

and

$$(K_{att} n_0 n_{e0} - K_{rec}\alpha_0^2 n_{e0}^2)\ell_p + \frac{7}{15} K_{rec}\alpha_0^2 n_{e0}^2 d = 0. \tag{60}$$

We need to determine $\Gamma_+(\text{wall})$ and obtain a third equation for the parameter d. To obtain $\Gamma_+(\text{wall})$ we note from the numerical results that even at the highest pressures $D_{a+} \cong (1 + T_-/T_+)D_+$ at the wall, thus

$$\Gamma_+(\text{wall}) = 2(1 + T_-/T_+)D_+\alpha_0 n_{e0}/d \tag{61}$$

To obtain a relation for d we return to our fundamental flux equation (1) for Γ_-. Noting that the flux due to the electric field is given approximately by the first term in (60), then this must be balanced by the diffusion flux in the strong gradient region to bring $\Gamma_-(\ell_p)$ to zero. Thus the second term in (60) must equal the diffusion flux which gives

$$2D_-\alpha_0 n_{e0}/d = \frac{7}{15} K_{rec} n_{e0}^2 \alpha_0^2 d. \tag{62}$$

Equations (59), (60) and (62) can then be solved simultaneously for T_e, α_0 and d. We have done this and the results are included in table 1. In figure 5 we compare the profiles obtained, using this model, with the profiles obtained by solution of the coupled equations (5) and (6) for the two higher pressure cases. We see that our heuristic model works quite well in the range of α_0 for which (22) is not satisfied so that the simple parabolic model is not a good approximation. The equations of the heuristic model join smoothly onto the parabolic model when $d = \ell_p$, such that (59) and (60) reduce to (37*a*) and (37*b*). For lower values of α_0 a choice must be made between the approximate global model and the more accurate three parameter parabolic model using (30), (32) and (33). If the latter choice is made there is a small discontinuity between the two solutions, since $\ell \neq \ell_p$ for the parabolic solution. This discontinuity disappears if a Bohm flux boundary condition is used in the high-α region. We have investigated this model and found results close to the model presented here.

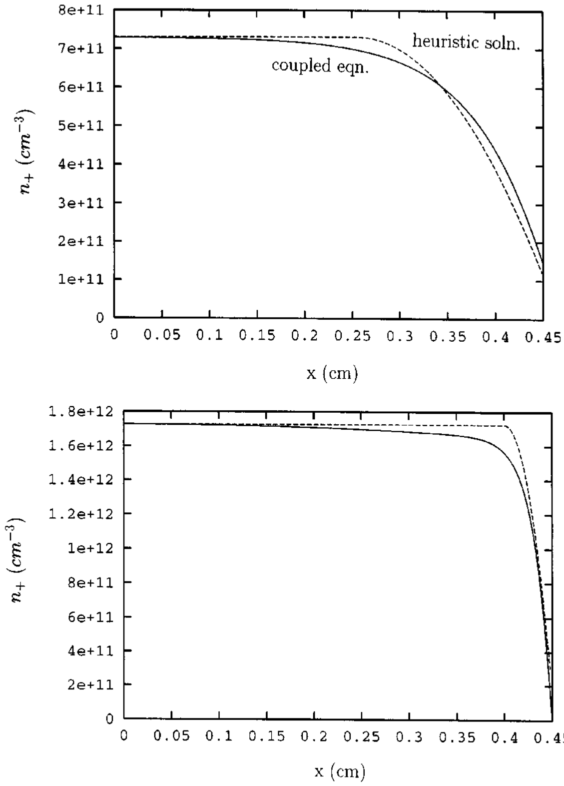

Figure 5. Comparison of n_+ profiles of the heuristic solution (dashed curves) to the numerical solutions of the coupled differential equations (solid curves). Top, p = 300 mTorr. Bottom, p = 2 Torr.

6. Conclusions and discussion

We have obtained equations that describe an electronegative plasma at high α when the edge region in which the plasma is electropositive becomes small. The electrons can always be taken to be in Boltzmann equilibrium. A pair of coupled differential equations are required to fully describe the equilibrium. These equations are valid over all parameters ranges, provided that the drift velocity of the positive ions does not reach the ion sound velocity within the plasma. The negative ions may or may not be described by the Boltzmann approximation, depending on the parameters. A single positive ion diffusion equation has been derived in the parameter range for which the Boltzmann approximation is valid for negative ions. We obtained a simple criterion to determine when the Boltzmann approximation is valid for negative ions. If the negative ions are not Boltzmann, an intermediate α regime exists for which the electron distribution is essentially flat such that the coupled differential equations can still be reduced to a single differential equation that can be solved in terms of elliptic integrals. An estimate of the breakdown of this solution has also been made.

Approximate equations were derived by assuming a parabolic solution for the negative ions. This solution is a good approximation for lower values of the electronegativity ratio $\alpha_0 = n_{-0}/n_{e0}$, where the diffusion flux dominates the recombination flux, but is not generally valid in the higher electronegativity parameter ranges that are the main subject of this paper. Nevertheless, the ansatz of a parabolic profile provides a simple method of estimating average plasma parameters of the electronegative equilibria, without solving differential equations. We compared the approximate solutions, using a parabolic profile, and using an elliptic profile, with the solution of the coupled differential equations. Within the range of validity of the two approximate solutions the results are quite similar to those obtained from the coupled differential equations. Moreover, even if the more exact solution is considerably flattened from a parabola, the average plasma parameters, using the parabolic approximation, are not very different from the average parameters obtained from the coupled equations. The comparisons of the various approximate solutions also show that the average plasma parameters and the scaling with control parameters can be reasonably approximated from a global model in which a parabolic profile with $\ell = \ell_p$ is assumed. We have utilized this approximation in a companion study [11] to explore the variation of average plasma parameters with control parameters, for a particular discharge configuration corresponding to a commercial reactor.

From the comparison of the numerical results to the various approximations, we determined that a heuristic model consisting of a flat central region and parabolic edges could well approximate the high-α region, both where the elliptic approximation is valid and at higher values of α where two coupled differential equations are required to obtain the solution. We compared the results obtained from the heuristic model with the solution of the coupled equations, finding good agreement. In the heuristic model, there is a smooth transition to a parabolic profile with decreasing electronegativity.

This paper has only been concerned with the high-α parameter range in which the electropositive edge plasma is sufficiently small that it can be neglected in the calculation. At lower α we have previously treated cases in which the electropositive halo was an essential part of the problem [3, 7, 9]. If we wish to connect the high and low α parameter regimes this can be done by including the electropositive edge, as described in section 3.3, in the model. Solution of the coupled differential equations, with a Bohm flux boundary condition, automatically includes an electropositive edge region, if it exists.

In finding the transitions between the various regimes, with increasing α, for our high-α solutions, we have essentially varied a single parameter (say n_0 or n_{e0}). In fact, the full problem is a function of both of these parameters, corresponding to the external parameters of pressure and power, mediated by the coefficients of a particular gas. If we span the two-dimensional parameter space, including low α solutions, the transitions are more complicated. In previous work [3,7,9] we have explored other parts of the parameter space. The complete exposition, covering the entire two-dimensional parameter space, is yet to be done.

Although we have generally considered that the solution of the coupled equations (5) and (6) give a fairly complete picture of the solutions for the purposes of this paper, this is not entirely correct. Particularly at lower pressures, but at reasonably high α, reaching the local Bohm velocity internally within the plasma leads to an abrupt transition to a lower density electropositive plasma [9]. In this paper we have taken this edge region to be sufficiently small that the boundary condition of a local Bohm velocity was taken to occur at $x = l_p$, rather than at $x = l_- < l_p$. It is possible to match the solution of the coupled equations to an edge electropositive solution, similar to that used for the parabolic approximation in section 3. As discussed in the introduction, l_p is not totally defined unless we know the method of plasma production. Thus in the example of section 4, the plasma dimension of 0.9 cm assumed nominal ion sheath widths in a symmetric rf capacitive discharge of approximately $s \simeq 0.5$ cm. The reduction of the electronegative core to accommodate a small electropositive edge would not be justified if the uncertainty in the sheath thickness is of the same order as the thickness of the electropositive layer.

Finally, we must recognize that particular plasmas may have special characteristics that are not covered within a generic analysis. For example, in [7] we compared our equilibrium results to a particle-in-cell (PIC) simulation of an rf capacitive discharge at relatively low pressure in oxygen. Some discrepancies in the equilibrium parameters were explained by the generation of a high temperature tail on the cooler bulk Maxwellian plasma, due to stochastic sheath heating. Our higher pressure example should not be severely subject to this phenomenon. Another limitation of the analysis occurs at high pressure, at which the electron temperature is not uniform over the discharge. This leads to peaking of the ionization and possibly peaking of the ion density near the plasma edge [14, 15]. We mentioned that this phenomenon might occur at the highest pressure of 2 Torr, in the example. Under certain circumstances it is also possible that our basic assumption of Boltzmann electrons breaks down. An example of this is a pulsed plasma in the afterglow, when essentially all of the electrons have escaped, and the negative ions are free to flow to the walls [16, 17]. New analysis is needed in this dramatically different regime.

Appendix A

The elliptic approximation is valid if the second LHS term in (26) is much smaller than the first left hand side term, i.e.

$$\left| \frac{\gamma \, \mathrm{d}^2 n_e/\mathrm{d}x^2}{2\mathrm{d}^2 n_+/\mathrm{d}x^2} \right| \ll 1 \tag{A1}$$

The second derivative of the ion density will be found below using the elliptic solution. The minimum value of $\mathrm{d}^2 n_+/\mathrm{d}x^2$ is located in the discharge centre. As will be shown, the second derivative of the electron density does not depend on x over most of the discharge. Therefore, condition (A1) is first violated at the discharge centre.

A.1. Expansion of the elliptic solution

Substituting β_0 from (48) and η from (51) into (50) yields

$$x = \left(\frac{3D_i}{2K_{rec} n_{e0} \alpha_0} \right)^{1/2} \int_{y(x)}^{1} \frac{\mathrm{d}y}{[(b-y)(1-y)(a+y)]^{1/2}} \tag{A2}$$

where $y(x) = \alpha(x)/\alpha_0$, and we have set $D_- = D_+ \equiv D_i$ and $T_- = T_+$. When recombination flux dominates flux to the walls η is very close to unity, but still $\eta < 1$. It follows from (52) that in this case $b = 1 + \epsilon$ and $a = 2 + \epsilon$ with $\epsilon \ll 1$. It is assumed here that T_e and η depend weakly on a particular realization of the boundary conditions. This allows one to use a zero boundary condition at the wall, $y(l_p) = 0$, instead of the Bohm condition. Substituting this into (A2) yields

$$\left(\frac{2K_{rec}n_{e0}\alpha_0\ell_p^2}{3D_i}\right)^{1/2} = \int_0^1 \frac{\mathrm{d}y}{[(1+\epsilon-y)(1-y)(2+\epsilon+y)]^{1/2}} \equiv J(\epsilon) \quad \text{(A3)}$$

The change of variable $t = 1 - y$ gives

$$J(\epsilon) = \int_0^1 \frac{\mathrm{d}t}{[t(t+\epsilon)(3+\epsilon-t)]^{1/2}} \quad \text{(A4)}$$

It is seen that this integral diverges logarithmically at the lower limit as $\epsilon \to 0$. In order to find the dominant term, $J(\epsilon)$ is written as

$$J(\epsilon) = \int_0^1 \frac{\mathrm{d}t}{\sqrt{3t(t+\epsilon)}} + \int_0^1 \frac{1}{\sqrt{t(t+\epsilon)}}\left\{\frac{1}{\sqrt{3+\epsilon-t}} - \frac{1}{\sqrt{3}}\right\}\mathrm{d}t. \quad \text{(A5)}$$

The first integral on the RHS can be calculated by substituting $t = w^2$. This results in

$$J_1 = \frac{2}{\sqrt{3}} \ln \frac{1+\sqrt{1+\epsilon}}{\sqrt{\epsilon}} \simeq \frac{1}{\sqrt{3}} \ln \frac{4}{\epsilon}. \quad \text{(A6)}$$

Since the second integral on the RHS remains finite as $\epsilon \to 0$, small terms of the order of ϵ can be omitted which yields

$$J_2 \simeq \int_0^1 \frac{\mathrm{d}t}{3\sqrt{1-t/3}(1+\sqrt{1-t/3})} = 2\ln\frac{2}{1+\sqrt{2/3}}. \quad \text{(A7)}$$

Adding J_1 and J_2 leads to

$$J(\epsilon) = \frac{1}{\sqrt{3}} \ln \frac{4}{\epsilon} + 2\ln\frac{2}{1+\sqrt{2/3}} \simeq \frac{1}{\sqrt{3}} \ln \frac{5.58}{\epsilon}. \quad \text{(A8)}$$

Substituting (A8) into (A3) yields

$$\epsilon = 5.58 \exp\left\{-\left(\frac{2K_{rec}n_{e0}\alpha_0\ell_p^2}{D_i}\right)^{1/2}\right\}. \quad \text{(A9)}$$

Indeed, ϵ becomes very small when the recombination flux becomes much larger than the diffusion flux. The parameter η can be found by substituting $b = 1 + \epsilon$ into (52), giving

$$\frac{1}{\eta} = 1 + \epsilon. \quad \text{(A10)}$$

It is now easy to obtain the second derivative of the ion density in the discharge centre. Substituting (51) into (25) we obtain

$$-2D_i \frac{\mathrm{d}^2 n_+}{\mathrm{d}x^2} = 2K_{rec}n_{e0}^2\alpha_0^2\left(\frac{1}{\eta} - 1\right) \simeq 11.16 K_{rec}n_{e0}^2\alpha_0^2 \times \exp\left\{-\left(\frac{2K_{rec}n_{e0}\alpha_0\ell_p^2}{D_i}\right)^{1/2}\right\} \quad \text{(A11)}$$

where (A9) and (A10) have been used to eliminate η in the second equality.

A.2. Electron density variation

Subtracting (8) from (7) gives

$$-2\gamma D_i \frac{\mathrm{d}}{\mathrm{d}x}\left(\frac{n_+}{n_e}\frac{\mathrm{d}n_e}{\mathrm{d}x}\right) = (K_{iz} - K_{att})n_0 n_e \quad \text{(A12)}$$

where $n_+/n_e \gg 1$ has been used. If n_+ and n_e vary little over most of the discharge we can substitute $n_+ = n_{+0} + \delta n_+$, $n_e = n_{e0} + \delta n_e$ and keeping only first order terms in δn_+ and δn_e we obtain

$$-2\gamma D_i \alpha_0 \frac{\mathrm{d}^2(\delta n_e)}{\mathrm{d}x^2} = (K_{iz} - K_{att})n_0 n_{e0}. \quad \text{(A13)}$$

The second term on the LHS in (26) can then be written as

$$-\gamma D_i \frac{\mathrm{d}^2 n_e}{\mathrm{d}x^2} = \frac{(K_{iz} - K_{att})n_0 n_{e0}}{2\alpha_0} \quad \text{(A14)}$$

It follows from this expression that $\mathrm{d}^2 n_e/\mathrm{d}x^2$ is approximately constant, which we use to find the maximum value of κ in the discharge.

The reaction rate K_{iz} depends strongly on the electron temperature, so we cannot use (A14) directly in (A1). We can eliminate this strong temperature dependence using the approximations of section 5. If recombination loss is much larger than loss to the walls the ion density is essentially flat in the central region of the discharge and varies mostly near the wall inside a region of a small width d. We can then use the profile in (58) to obtain (60). As argued there, the first term on the LHS of (60) can be attributed to the negative ion flux due to the electric field, and the second term to the negative ion diffusion flux at the wall. This interpretation yields (62) which can be solved for d giving

$$\frac{d}{\ell_p} = \left(\frac{30D_i}{7K_{rec}n_{e0}\alpha_0\ell_p^2}\right)^{1/2}. \quad \text{(A15)}$$

It can now be seen that the central region where n_+ is flat expands (d decreases) as the ratio of the recombination loss to the diffusion loss increases. Subtracting (59) and (60) with $\Gamma_+(\text{wall}) = 4D_i\alpha_0 n_{e0}/d$ from (61) gives

$$4D_i\alpha_0 n_{e0}/d = (K_{iz} - K_{att})n_0 n_{e0}\ell_p. \quad \text{(A16)}$$

Substituting d from (A15) into (A16) yields

$$(K_{iz} - K_{att})n_0 n_{e0} = 4\alpha_0 n_{e0}\left(\frac{7K_{rec}n_{e0}\alpha_0 D_i}{30\ell_p^2}\right)^{1/2}. \quad \text{(A17)}$$

Substituting (A17) into (A14) then gives

$$-\gamma D_i \frac{\mathrm{d}^2 n_e}{\mathrm{d}x^2} = n_{e0}\left(\frac{28K_{rec}n_{e0}\alpha_0 D_i}{30\ell_p^2}\right)^{1/2}. \quad \text{(A18)}$$

This equation's RHS contains only quantities which depend weakly on T_e.

A.3. Criterion

Dividing (A18) by (A11) the criterion (A1) at the discharge centre can be written as

$$\kappa \equiv \frac{1}{11.55\alpha_0}\left(\frac{D_i}{K_{rec}n_{e0}\alpha_0\ell_p^2}\right)^{1/2} \times \exp\left(\frac{2K_{rec}n_{e0}\alpha_0\ell_p^2}{D_i}\right)^{1/2} < 1 \qquad \text{(A19)}$$

where a simple, rather than a strong inequality is used, since the LHS is the largest value that the inequality, defined in (A1), attains.

Acknowledgments

The authors wish to acknowledge the support of Department of Energy Grant DE-FG03-87ER13727, National Science Foundation Grant ECS-921750, Department of Energy Grant PPRI-LLNL CP 94-06/B28326, and a gift from the Lam Research Corporation. The Russian authors wish to acknowledge the support of INTAS Grant N94-0740. IDK acknowledges the Alexander von Houmboldt foundation for a research fellowship.

References

[1] Edgley P D and Von Engel A 1980 *Proc. R. Soc.* A **370** 375

[2] Ferreira C M, Gousset G and Touzeau M 1988 *J. Phys. D: Appl. Phys.* **21** 1403
Ferreira C M and Gousset G 1991 *J. Phys. D: Appl. Phys.* **24** 775

[3] Tsendin L D 1989 *Sov. Phys.—Tech. Phys.* **34** 11

[4] Kaganovich I D and Tsendin L D 1993 *Plasma Phys. Rep.* **19** 645

[5] Haas F A, Lea L M and Holmes A J T 1991 *J. Phys. D: Appl. Phys.* **24** 1541

[6] Franklin R N, Daniels P G and Snell J 1993 *J. Phys. D: Appl. Phys.* **26** 1638

[7] Lichtenberg A J, Vahedi V, Lieberman M A and Rognlien T 1994 *J. Appl. Phys.* **75** 2339

[8] Lee C, Graves D B, Lieberman M A and Hess D W 1994 *J. Electrochem. Soc.* **141** 6
Lee C and Lieberman M A 1995 *J. Vac. Sci. Technol.* A **13** 368

[9] Kouznetsov I G, Lichtenberg A J and Lieberman M A 1996 *Plasma Sources Sci. Technol.* **5** 662

[10] Lieberman M A and Lichtenberg A J 1994 *Principles of Plasma Discharges and Materials Processing* New York: Wiley

[11] Lee Y T, Lieberman M A, Lichtenberg A J, Bose F, Baltes H and Patrick R 1997 Global model for high pressure electronegative chlorine/helium discharges *J. Vac. Sci. Technol.* to be published

[12] Thompson J B 1959 Research notes *Proc. R. Soc.* **73** 818
Rogoff G L 1985 *J. Phys. D: Appl. Phys.* **18** 1533

[13] Boyd R L F and Thompson J B 1959 *Proc. R. Soc.* A **252** 102
Riemann K-U 1991 *J. Phys. D: Appl. Phys.* **24** 493
Boswell R W, Lichtenberg A J and Vender D 1992 *IEEE Trans. Plasma Sci.* **PS-20** 62

[14] Schweigert V A 1991 *Sov. J. Plasma Phys.* **17** 844

[15] Kaganovich I D 1995 *Plasma Phys. Rep.* **21** 434

[16] Smith D, Dean A G and Adams N G 1974 *J. Phys. D: Appl. Phys.* **7** 1944

[17] Ashida S and Lieberman M A 1997 *Japan. J. Appl. Phys.* to be published